minerals

Article

Mineral Liberation and Concentration Characteristics of Apatite Comminuted by High-Pressure GRU

Yongbo Fan [1,*,†], Genghao Zhang [2,†], Shihai Li [1,*], Li Zhang [1], Jianqiang Guo [1] and Chun Feng [1]

[1] Key Laboratory for Mechanics in Fluid Solid Coupling Systems, Institute of Mechanics, Chinese Academy of Sciences, Beijing 100045, China; lizhang@imech.ac.cn (L.Z.); gjq_ustb@163.com (J.G.); fengchun@imech.ac.cn (C.F.)
[2] School of Civil and Resource Engineering, University of Science and Technology Beijing, Beijing 100083, China; zhanggenghao210727@163.com
* Correspondence: ybfan@imech.ac.cn (Y.F.); shli@imech.ac.cn (S.L.)
† These authors contributed equally to this work.

Abstract: Mineral liberation and concentration have always been the core issues in ore processing. The goal of multi-stage crushing and ball milling is liberation because mineral liberation is the foundation of beneficiation. High energy consumption and environmental pollution have always been unavoidable topics. We put forward the method of high-pressure gas rapid unloading (GRU). Particle size followed MR-R distribution. The scanning electron microscopy data showed that the liberation of apatite particles smaller than 4 mm was sufficient by high-pressure GRU methods, and high-grade apatite concentrated in the particle size range of 0.5 to 4 mm. The average grade of the preferred particle size interval was 3%–5% higher than the original ore. Liberation degrees of apatite less than 4 mm are above 88%, which was beneficial for mineral processing. Compared to the traditional crushing method, the GRU method had a higher liberation and concentration in the particle size range of 0.5 to 4 mm. The total energy consumption was about 1.76 kW·h/t, less than that of the traditional crushing method.

Keywords: apatite; mineral liberation; mineral concentration; preferred particle size interval

check for updates

Citation: Fan, Y.; Zhang, G.; Li, S.; Zhang, L.; Guo, J.; Feng, C. Mineral Liberation and Concentration Characteristics of Apatite Comminuted by High-Pressure GRU. *Minerals* **2024**, *14*, 1148. https://doi.org/10.3390/min14111148

Academic Editors: Rodrigo Magalhães de Carvalho, Zhiyong Gao, Zhao Cao, Jian Cao, Shihong Xu and Zhitao Feng

Received: 10 September 2024
Revised: 23 October 2024
Accepted: 11 November 2024
Published: 13 November 2024

1. Introduction

Apatite is a group of natural calcium, mineral fluorine, and chlorine ($Ca_5(PO_4)_3$(F, Cl, OH)). The most common forms of apatite are fluorapatite ($Ca_5(PO_4)_3(F)$), hydroxyapatite ($Ca_5(PO_4)_3(OH)$), and chlorapatite ($Ca_5(PO_4)_3(Cl)$ [1] The mineral primarily occurs as phosphate rock. Apatite is considered a source of phosphorus, phosphoric acid, and fertilizers. China is extremely rich in phosphate mineral resources, just behind South Africa and Morocco, accounting for third place in the world's phosphorus resources. Although China has a large amount of apatite ore resources, as illustrated in Figure 1, the average grade of apatite ore is only 16.95%, and only 6.75% are rich ores with P_2O_5 grades larger than 30% (857 million tons). The beneficiation of low-grade apatite has been necessary for decades [2,3].

Mineral liberation is the fundamental problem of mineral processing [4]. A principal purpose of comminution in mineral processing is liberation [5,6]. The relationship between size and grade is quite understandable, as large particles tend to have grades close to the average ore grade. In contrast, finer particles are respectively close to 0% or 100% grade [7]. If each particle contains a single mineral, individual minerals are separated. However, sufficient mineral liberation is extremely difficult to reach [8–10]. Indeed, the particle liberation degree is the crucial variable to define the performance of any separation technology [11–13].

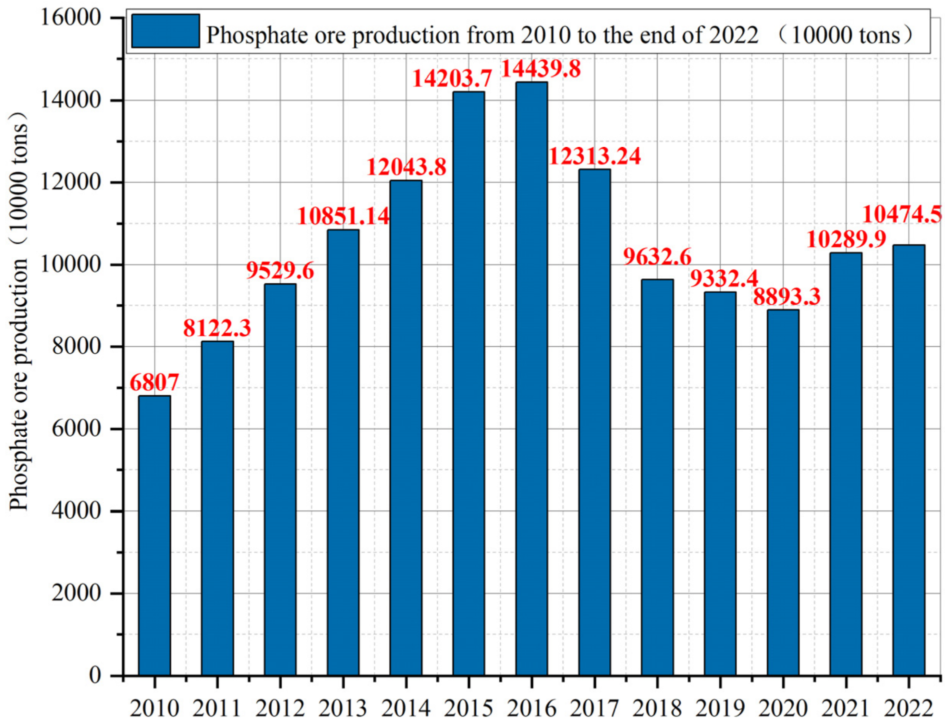

Figure 1. Apatite ore production of China, 2010–2022.

The limitations of conventional comminution technology have been reviewed by Wills [14], who found that it was desirable to devise improved methods that applied the breaking force preferentially at mineral grain boundaries rather than randomly as in a conventional tumbling mill. It is highly beneficial to achieve liberation by grain boundary fracture. This theme was well-established in the mineral processing research literature.

Traditional multistep crushing, grinding, and flotation technologies have significantly developed in the last few hundred years because the liberation of the target mineral was already sufficiently high with particle size reduction [15–17]. Particulate materials are fractured primarily by compressive stress. Subsidiary fracture is caused by high shearing stress, particularly at the particle surface. Patterns of fracture by mechanical comminution mainly include shatter, cleavage, attrition, and chipping. The fracture patterns of conventional crushing equipment (jaw crusher, cone crusher, etc.) are impact and cleavage [6]. The traditional compression and shear crushing method achieves sufficient liberation only by particle size reduction. The energy consumed increases significantly because of the surface area [18–21].

Ball milling has the following characteristics: (a) “partial” loading and “external” loading; (b) overcoming the compressive strength or shear strength. Compression shear is the main failure style during the ball milling process. Compared with the ball milling method, pulverizing ore by the high-pressure GRU method has the following characteristics: (a) “uniform” loading and “internal” gas infiltration loading; (b) overcoming the tensile strength conserved much energy [22]. Besides this, the method results in absolute physical separation.

Considering the diverse compositions, texture, and other physio-chemical properties of the natural apatite ore, numerous beneficiation processes have been investigated [23–26]. Low-grade apatite ore upgraded the ore grade by several mineral processing methods, including flotation, magnetic separation, density separation, and electrostatic separation, which were all efficient enrichment approaches [27–31]. Flotation technology is widely used in mineral processing [32]. Density separation, electrostatic separation, and magnetic separation technologies have all been investigated. However, these techniques have limited application because of high power input and limited capacity constraints. Calcination is mostly used in ore processing for lime processing [33].

Apatite is commonly associated with dolomite and Fushan stone and usually appears with interlayers. Moreover, its density difference is less than 0.3 g/cm^3, so, it is highly arduous to complete mineral processing through density separation. When the thickness of the interlayer between apatite and shale or dolomite is only 5 mm or less, density separation is especially ineffective, so interlayered apatite ore needs to be crushed to a particle size smaller than 0.074 mm by ball milling and separated by flotation or reverse flotation to obtain P_2O_5. In this case, the cost increases significantly.

This article proposes the pulverization method of high-pressure GRU for micron-sized apatite powder production. In this paper, the authors designed a series of ore pulverization experiments to explore the liberation and concentration of apatite. Furthermore, the particle size distribution curve complied with the modified R-R function.

2. Materials and Methods

The ore powder was dried and sieved to obtain the particle size distribution. The sieve diameter included eight groups: 0.045 mm, 0.074 mm, 0.147 mm, 0.5 mm, 1 mm, 1.43 mm, 2 mm, and 4 mm.

2.1. Materials and GRU Methods

We weighed the ore before putting it into the high-pressure infiltration chamber. The equivalent diameter of the apatite ore was <60 mm because the inner diameter of the high-pressure infiltration chamber was 63 mm. The inner volume of the high-pressure infiltration chamber was approximately 0.003 m^3, and according to the volume ratio of densely packed particles of equal diameter, the porosity was approximately 35%–40%; therefore, the mass of the apatite ore was about 3 kg. The pressures of the high-pressure propulsion chamber and high-pressure infiltration chamber were 22 MPa and 25 MPa, respectively. After sealing, air filling, air substitution, and high water pressure initialization, the high-pressure infiltration chamber was placed in the collection container to collect the apatite ore powder; the apparatus is illustrated in Figure 2. Eventually, the rupture disk burst, and the apatite ore powder sprayed into the collection container.

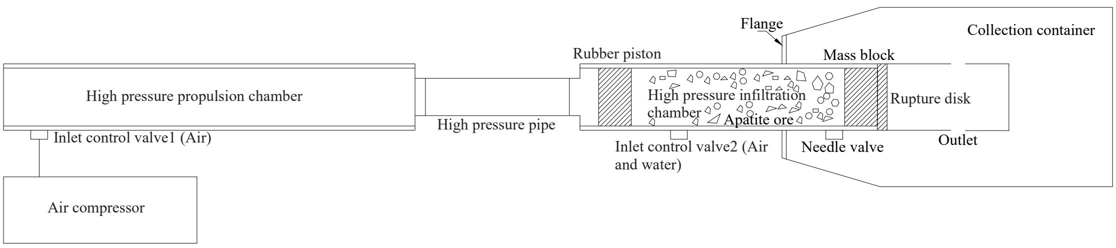

Figure 2. Schematic diagram of experimental apparatus.

Currently, the overall process includes air filling in the high-pressure infiltration chamber and high-pressure propulsion chamber, air substitution in the high-pressure infiltration chamber, and rapid unloading of air in the high-pressure infiltration chamber.

First, the high-pressure propulsion chamber was connected to the high-pressure infiltration chamber by a pipe. Between the two chambers, there was a rubber piston, which was responsible for full-section propulsion. Second, we placed apatite ore into the high-pressure infiltration chamber. After sealing, we injected high-pressure air. Third, dissociative air between the apatite ore was substituted by water and collected for cyclic utilization. Fourth, apatite ore and water spouted out of the high-pressure infiltration chamber propelled by air in the high-pressure propulsion chamber, based on the rapid unloading actuated by the rupture disk's bursting.

2.2. BPMA Methods

BPMA (BGRIMM Process Mineralogy Analyzer) is an automatic analysis system for process mineralogy. The BPMA system consists of a scanning electron microscope

(SEM), an energy dispersive spectrometer (EDS), and a set of process mineralogy automatic testing software (BPMA V1.0), as shown in Figure 3. Compared with similar commercial software used internationally such as MLA, AMICS, and TIMA, BPMA has unique technical characteristics, manifesting in accurate adhesion particle segmentation effect and efficiency, precise mineral phase extraction ability, a complete theoretical mineral energy spectrum database, and powerful target particle searchability.

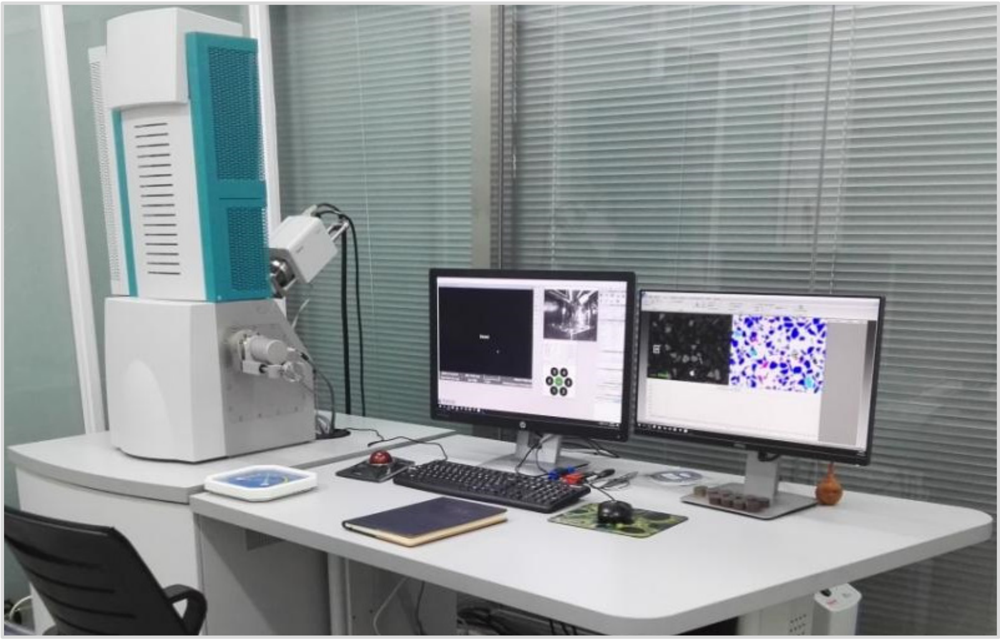

Figure 3. BGRIMM Process Mineralogy Analyzer (BPMA).

3. Results

3.1. Particle Size Follows MR-R Distribution

The most common mathematical models utilized to describe the experimental particle size distribution (PSD) of curves are the R-R function and Gates–Gaudin–Schuhmann (GGS) [33]. Among them, the R-R function was probably the most suitable to describe the PSD. The general expression of the R-R function is illustrated in to Equation (1). The expression of the Modified R-R function is illustrated in Equation (2) because the maximum particle size is not infinite (d_m is considered).

$$F(x) = 1 - e^{-\left(\frac{x}{\lambda}\right)^k}, 0 \leq x \leq +\infty \tag{1}$$

$$F(x) = 1 - e^{-\left(\frac{x}{\lambda}\frac{d_m-\lambda}{d_m-x}\right)^k}, 0 \leq x \leq d_m \tag{2}$$

where x is the particle size (mm), d_m is the maximum particle size (mm), λ is the particle size with a cumulative rate under sieve of 63.1%, representing the mean particle size, k is the non-uniformity coefficient, a measure of the spread of particle sizes, and $F(x)$ is cumulative rate.

Four group apatite pulverization experiments included high magnesium apatite ore, Sujiapo apatite ore, Yinjiaping apatite ore, and Chuan apatite ore. Correlation coefficient R^2 was, respectively, 99.8%, 99.8%, 99.2%, and 99.8%, as illustrated in Figure 4a–d.

Particle size distribution (PSD) of the particles obtained by high-pressure GRU conformed to a normal distribution, and cumulative PSD conformed to the Modified Rosin–Rammler function. The particles were continuous, and the minimum and maximum sizes of the particle after the high-pressure GRU were about 10–15 μm and 10–15 mm.

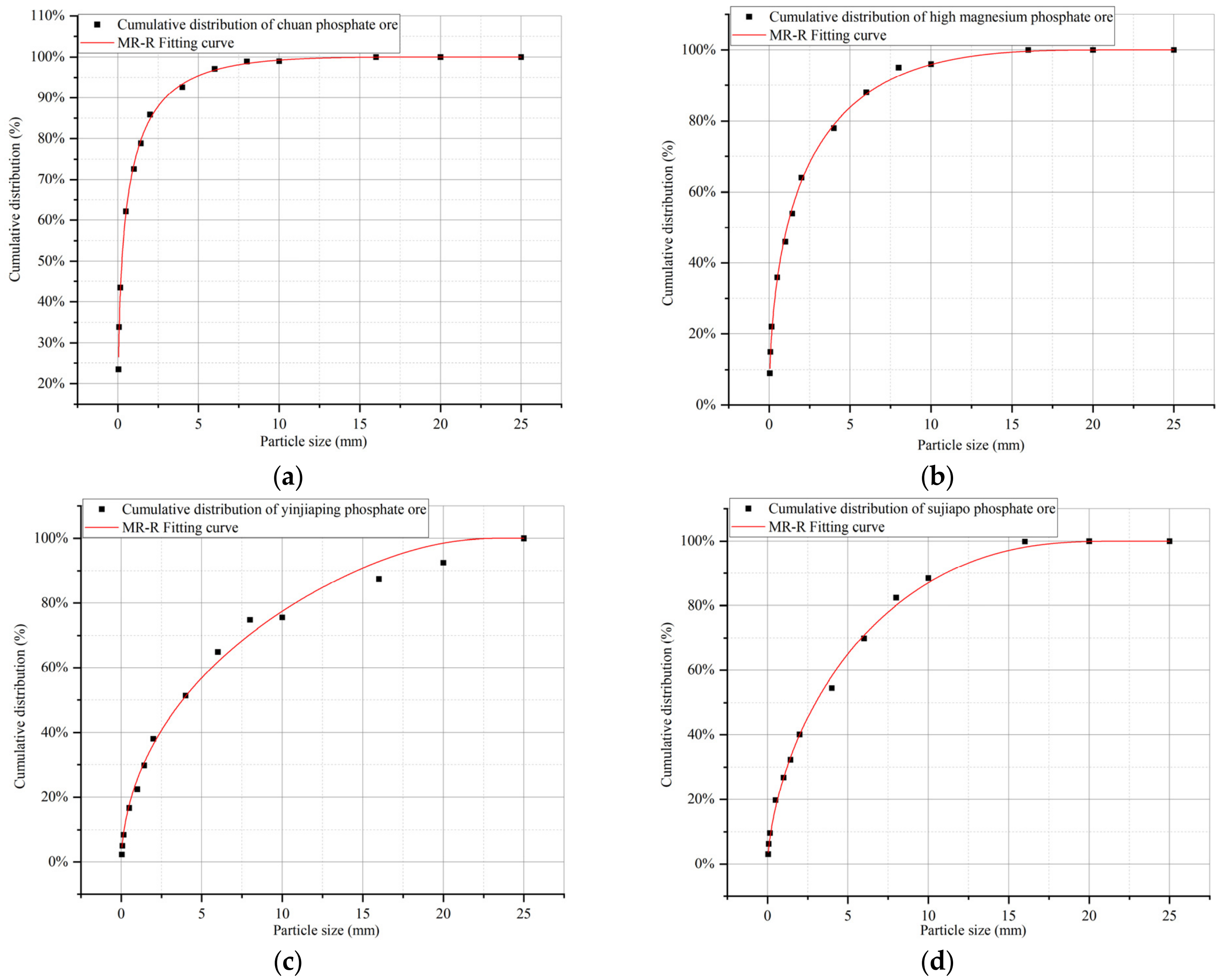

Figure 4. Fitting curve of different phosphate ores. (**a**) Chuan phosphate, (**b**) high magnesium phosphate, (**c**) Yinjiaping phosphate, (**d**) Sujiapo phosphate.

λ can be obtained from the MR-R function. Both of λ, infiltration pressure P_0, propulsion pressure P_t, tension strength σ_t, and shear strength σ_τ complied with a functional relation as follows:

$$\frac{d_m - \lambda}{\lambda} = A \cdot \frac{P_0}{\sigma_t} + B \cdot \frac{P_t}{\sigma_\tau} \tag{3}$$

P_0—infiltration pressure, P_t—propulsion pressure.

σ_t—tension strength, σ_τ—shear strength, A,B—coefficient, obtained by fitting.

3.2. Apatite Particles Smaller than 4 mm Completely Dissociated

After high-pressure GRU experiments, the powder obtained was dried and sieved. Each group of particles was analyzed, as illustrated in Figure 5. Particle distribution was assessed by scanning electron microscopy. The liberation of apatite particles smaller than 4 mm was sufficient. Impurities such as quartz, dolomite, and calcite were all attached to the apatite particles with fine-grained particles, and impurities with large particle sizes were relatively few, as illustrated in Figure 5a–c. Most impurities existed in clusters in fine-grained intervals smaller than 0.15 mm, and impurities with large particle sizes started increasing, as illustrated in Figure 5d–f.

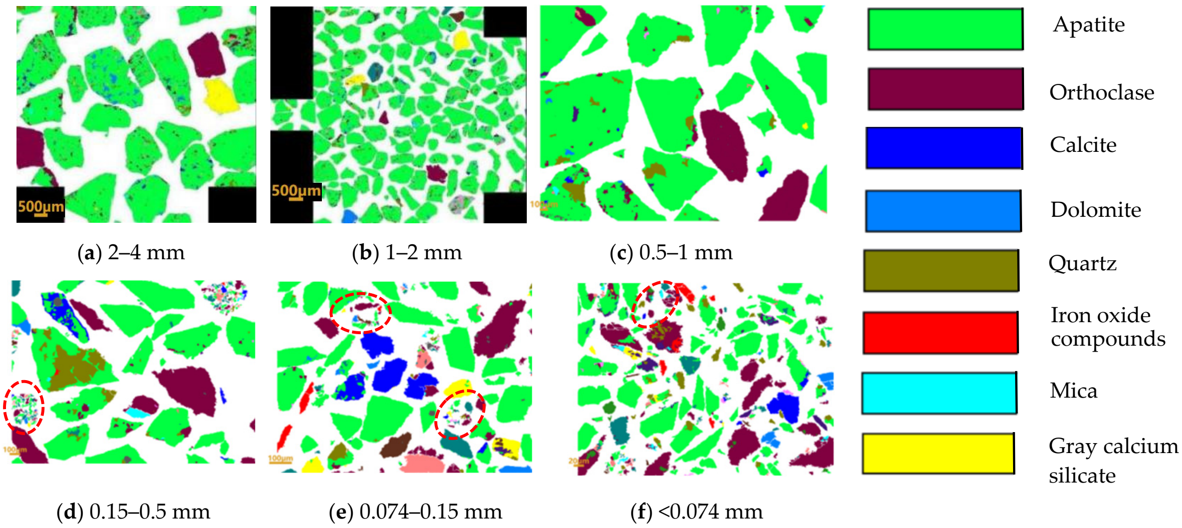

Figure 5. (**a**) SEM observation images of 2–4 mm apatite particles associated with multiple minerals; (**b**) SEM observation images of 1–2 mm apatite particles associated with multiple minerals; (**c**) SEM observation images of 0.5–1 mm apatite particles associated with multiple minerals; (**d**) SEM observation images of 0.15–0.5 mm apatite particles associated with multiple minerals; (**e**) SEM observation images of 0.074–0.15 mm apatite particles associated with multiple minerals; (**f**) SEM observation images of <0.074 mm apatite particles associated with multiple minerals.

Impurities appeared as fine particles and adsorbed on the surface of apatite minerals, and this was the core factor in reducing the grade in the preferred particle size range.

3.3. The Relationship of P_2O_5 Grade and Particle Size

The complete liberation of minerals was the most important outcome in the beneficiation process, and the uniform infiltration of high-pressure gas was the most crucial condition for facilitating sufficient liberation, compared to multi-stage crushing and ball milling.

The mineral composition of Yinjiaping apatite ore mainly included apatite and dolomite, and the two minerals appeared in interlayered style. The quality of apatite ore was about 3048 g, as illustrated in Figure 6a. The experimental apparatus and pressure combination were the same as in Section 2.1. After the first experiment, undissociated apatite ore continued to be processed. The remainder of ore quality of Yinjiaping apatite with interlayered style was only 285.6 g and 53.6 g after the first and the second experiments, accounting for 9% and 1.8% of the total quality of the apatite ore (as illustrated in Figure 6b,c), which indicated that the majority of interlayered apatite ore dissociated. The P_2O_5 grade of the original apatite ore was about 18.25%, and high P_2O_5 grade of apatite was distributed in the particle size interval of 0.5–5 mm, respectively, 20.86%, 21.44%, and 20.96% processed by high-pressure GRU. P_2O_5 grade of fine particle size less than 0.1 mm was 18.43%, as illustrated in Figure 6d and Table 1.

Table 1. P_2O_5 grade of Yinjiaping different particle size intervals.

Diameter (mm)	Quality Proportion (%)	P_2O_5 Grade of Different Intervals (%)	P_2O_5 Quality	P_2O_5 Grade (%)
>5	42.85%	14.62%	6.26%	14.62%
3–5	28.46%	20.96%	5.97%	
1–3	13.70%	21.44%	2.94%	21.06%
0.5–1	12.84%	20.86%	2.68%	
0.1–0.5	2.00%	18.21%	0.36%	18.38%
<0.1	7.10%	18.43%	1.31%	
The P_2O_5 grade of the original apatite ore		18.25%		

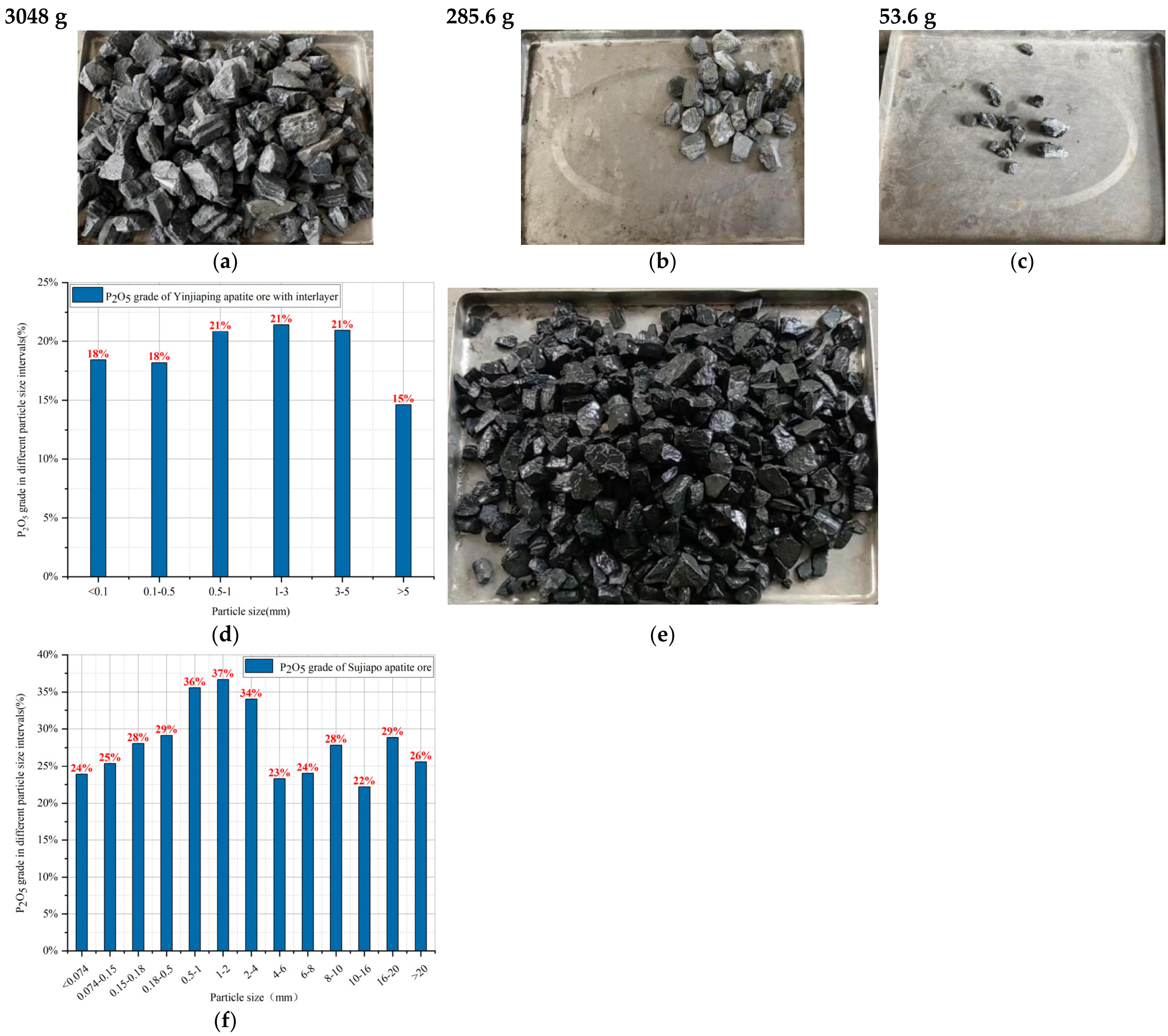

Figure 6. High-grade apatite concentrated in the specific particle size interval. (**a**) Apatite associated with dolomite, (**b**) apatite associated with dolomite after the first experiment, (**c**) apatite associated with dolomite after the second experiment, (**d**) P_2O_5 grade of Yinjiaping, (**e**) apatite associated with shale, (**f**) P_2O_5 grade of Sujiapo.

The mineral composition of Sujiapo apatite ore mainly included apatite and shale, as illustrated in Figure 6e. The P_2O_5 grade of the original apatite ore was about 28%. The experimental apparatus and pressure combination were the same as above. After the experiment, the high P_2O_5 grade of apatite was distributed in the particle size interval of 0.5–4 mm, respectively, 36%, 37%, and 34% after processing by high-pressure GRU. The P_2O_5 grade of fine particle size less than 0.15mm was 24%–25%, as illustrated in Figure 6f and Table 2.

In addition, the P_2O_5 grade of the particle size greater than 5 mm was lower by 2%–3% than that of the original ore, which revealed that apatite was separated from impurities and entered the preferred particle size interval.

The average P_2O_5 grade of the preferred particle size interval was 33.94%, as illustrated in Table 2. It was about 3%–5% higher than the original ore. Simultaneously, the average

P_2O_5 grade of fine particles was lower than the original ore. Most impurity minerals became fine particles and separated from the apatite.

Table 2. P_2O_5 grade of Sujiapo different particle size intervals.

Diameter (mm)	Quality Proportion (%)	P_2O_5 Grade of Different Intervals (%)	P_2O_5 Quality	P_2O_5 Grade (%)
>20	0.14%	25.61%	0.036%	23.45%
16–20	0.65%	28.85%	0.19%	
10–16	5.81%	22.20%	1.29%	
8–10	6.08%	27.85%	1.69%	
6–8	9.86%	24.03%	2.37%	
4–6	17.38%	23.29%	4.05%	
2–4	14.9%	34.04%	5.07%	33.94%
1–2	16.05%	36.69%	5.89%	
0.5–1	6.76%	35.58%	2.41%	
0.18–0.5	7.94%	29.12%	2.31%	
0.15–0.18	3.26%	28.07%	0.92%	
0.074–0.15	3.57%	25.38%	0.91%	24.40%
<0.074	7.25%	23.91%	1.73%	

Reducing the percentage of apatite in fine particles was the outstanding advantage of this method. Because the strength of apatite was higher than dolomite and shale, although their densities were similar, apatite was concentrated in the coarse-grained particles, while dolomite and shale were both distributed in the fine-grained particles, which was beneficial for the beneficiation process. It could be possible to achieve a tailings grade of less than 10% after extracting apatite from the fine particles.

3.4. Quality Proportion and Liberation Degree

The key to improving the P_2O_5 grade within the preferred particle size interval was to remove dolomite and shale. These impurities are easy to reduce to fine-grained particles because of their lower strength. The impurities separated from apatite and became fine-grained intervals, which was why the P_2O_5 grade in the preferred particle size interval was higher than that of the original ore.

Based on the experimental result of Section 3.3, the quality proportion and liberation degree were available. The ratio of molecular mass between P_2O_5 and apatite was 0.423. We can obtain the mass proportion of apatite in different particle size intervals, as illustrated in Figure 7a. The liberation degree is an indicator used to characterize the difficulty of mineral processing. When it is greater than 80%, it indicates that mineral processing is easy to achieve. As illustrated in Figure 7b, the liberation degree of apatite was greater than 88% in all particle size intervals less than 4 mm, indicating that the apatite sufficiently dissociated.

3.5. Liberation and Energy Consumption Compared to the Traditional Methods

3.5.1. Liberation Comparison

G28-L28 expresses that propelling and infiltration pressure were both 28 MPa. Yinjiaping apatite ore with a 5 mm dolomite interlayer is illustrated in Figure 8. We conducted a comparative experiment. Samples were the same as in Figure 6a. The results suggested that the particle size distribution pattern of apatite ore with dolomite interlayers crushed by traditional crushing was consistent with dolomite ore crushed by the GRU method. However, it was different from interlayered apatite ore crushed through the GRU method. The results indicated that the particle mass proportion caused by traditional crushing was less than that of the GRU methods in the particle size range of 0.5 to 4 mm. Based on Sections 3.2 and 3.3, the high P_2O_5 grade of apatite was among the particle size range of 0.5 to 4 mm. Compared to the traditional crushing method, the GRU method had a higher degree of liberation and concentration in the particle size range of 0.5 to 4 mm.

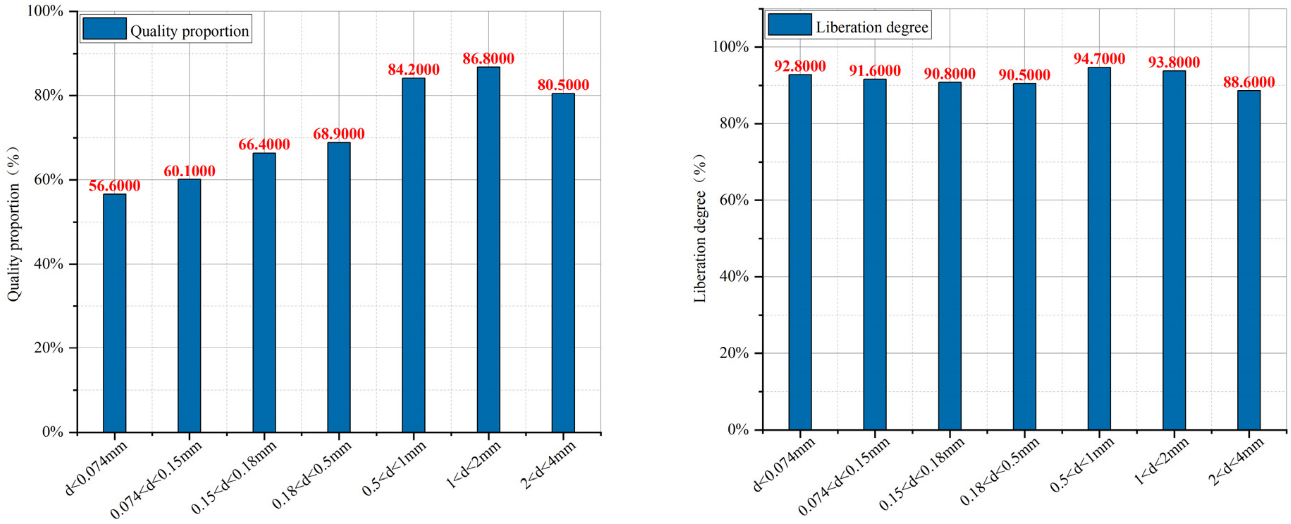

(**a**) (**b**)

Figure 7. Quality proportion and liberation degree of different particle size intervals of apatite. (**a**) Quality proportion. (**b**) Liberation degree.

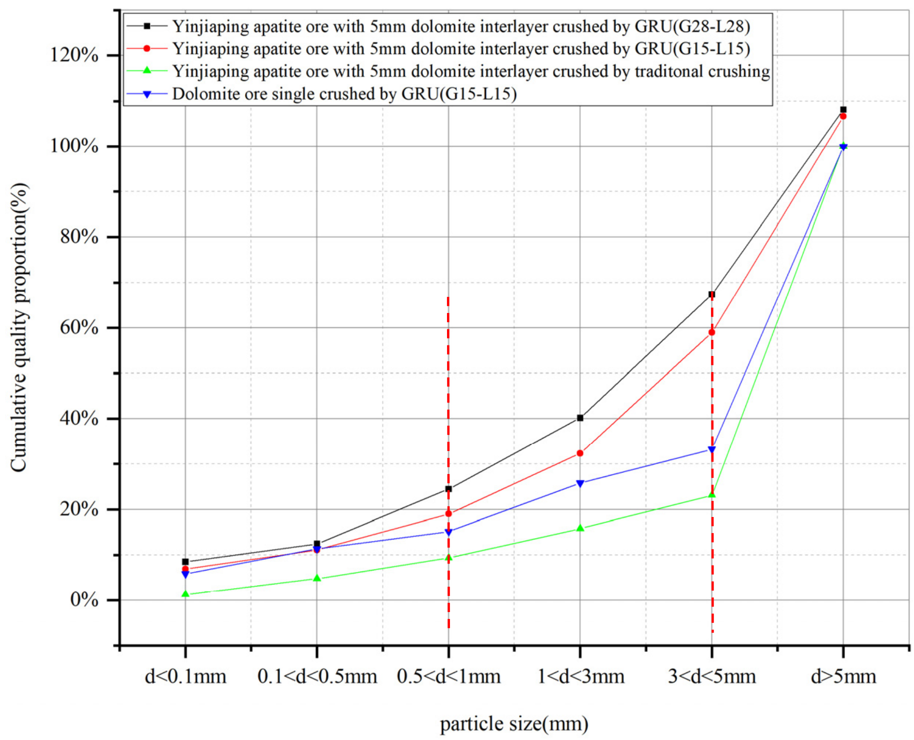

Figure 8. Comparative experiment between GRU method and conventional crushing method.

3.5.2. Energy Consumption Comparison

We conducted comparative experiments. The feed size of apatite ore is about 100 mm, and the discharge size of apatite was less than 20 mm. Energy consumption of the high-pressure GRU method included water pre-loading, gas substitution, gas propulsion, and rubber piston resetting. Each energy consumption was 0.96 kW·h/t, 0.0015 kW·h/t, 0.4 kW·h/t, 0.4 kW·h/t. The total was about 1.76 kW·h/t. The energy consumption of the traditional method is shown in Figure 9. Even if all particle sizes were about 20 mm, the energy consumption was about three kW·h/t.

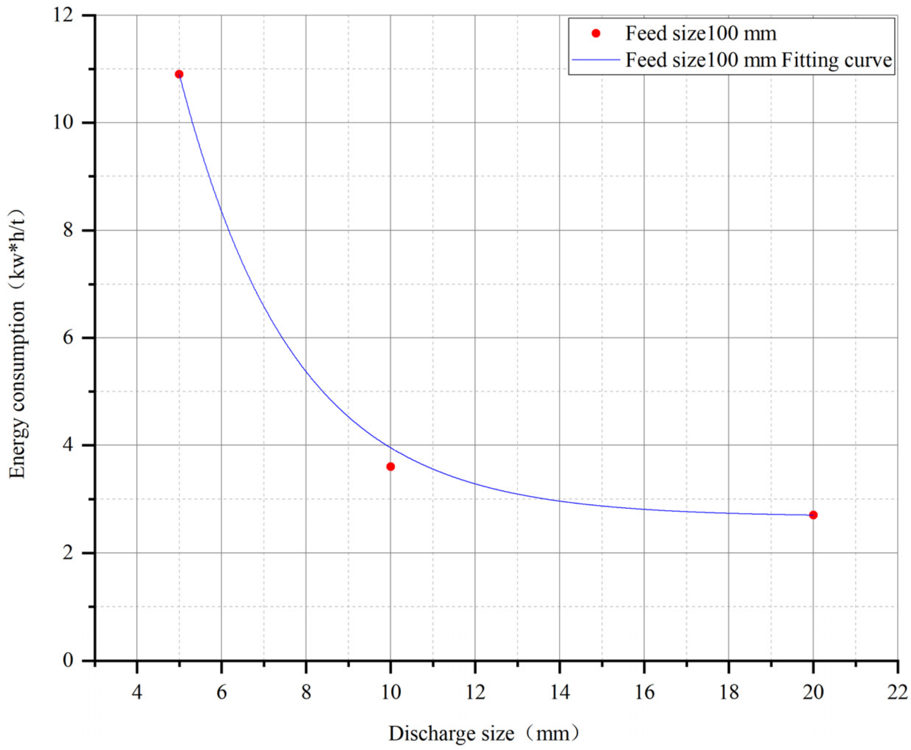

Figure 9. Energy consumption of traditional method.

4. Discussion

Because of the uniform permeation of high-pressure gas and its mechanism to overcome the tensile strength of ores, the high-pressure GRU method demonstrated characteristics of liberation by grain boundary fracture and low energy consumption. It was especially well-suited for porous, brittle materials. Mineral liberation and concentration helped significantly to reduce energy consumption in ore crushing.

Furthermore, high-pressure gas pushing high-pressure water and ore obtained mineral liberation. Since water is incompressible, it consumes less energy even if the water pressure is higher. As a result, there will be more opportunities for the high-pressure GRU (or water) method. Interlayered rocks are common in nature, especially in sedimentary rocks. Furthermore, most ores have a low grade and irregular mineral distribution, especially in China. Thus, further investigation into mineral concentration in mineral processing is warranted. Because the current procedures for dissociating interlayered ores are either complex or ineffective, many interlayered ores are treated as trash, which is a heavy loss.

The method promotes the transformation of existing material multi-stage crushing and ball milling processes and could facilitate the efficient development and utilization of global mineral resources. As a result, the high-pressure GRU method offers a potential remedy for the growing problems with mineral resources that many nations face globally.

5. Conclusions

The method induced tensile failure and comminuted the apatite ore into micron-sized particles. It tore apart minerals along the mineral bonding surface. High-pressure gas within the ore comminuted the ore along the mineral bonding surface or micro-cracks. It was the physical foundation of continuous particle size distribution produced by high-pressure GRU methods.

Cumulative PSD conforms to the Modified Rosin-Ramller function. The liberation of apatite particles smaller than 4 mm was sufficient by high-pressure GRU methods, and high-grade apatite concentrated in the particle size range of 0.5 to 4 mm. The average grade of the preferred particle size interval was 33.94%. It was about 3%–5% higher than the original ore. Liberation degrees of apatite less than 4 mm were above 88%, which was beneficial for mineral processing. Compared to the traditional crushing method, the GRU method had a higher liberation and concentration in the particle size range of 0.5 to 4 mm. The total energy consumption was about 1.76 kW·h/t, less than that of the traditional crushing method.

Author Contributions: S.L. performed the Conceptualization and methodology G.Z. performed data analysis; L.Z. performed the validation and data curation; J.G. performed the Investigation; C.F. provided funding acquisition. Y.F. wrote the manuscript. All authors have read and agreed to the published version of the manuscript.

Funding: The work presented in this paper was supported by the National Key Research Development Project (E3YF040301), and Chinese Academy of Sciences strategic leading science and technology project (E4XA040103, E4XA040451).

Data Availability Statement: The datasets used and/or analyzed during the current study are available from the corresponding author upon reasonable request.

Acknowledgments: The authors sincerely want to thank Guo WX, Liu HQ, and Luo Huan for their help with the laboratory equipment and extensive experiments. We are also grateful for the funding support from National Key Research Development Project.

Conflicts of Interest: We declare that we have no financial and personal relationships with other people or organizations that can inappropriately influence our work, and there is no professional or other personal interest of any nature or kind in any product, service, and/or company that could be construed as influencing the position presented in, or the review of, the manuscript entitled.

References

1. Dong, L.; Wei, Q.; Qin, W.; Jiao, F. Selective adsorption of sodium polyacrylate on calcite surface: Implications for flotation separation of apatite from calcite. *Sep. Purif. Technol.* **2019**, *241*, 116415. [CrossRef]
2. El-Shall, H.; Zhang, P.; Khalek, N.A.; El-Mofty, S. Beneficiation technology of phosphates: Challenges and solutions. *Mining, Met. Explor.* **2003**, *21*, 17–26. [CrossRef]
3. Kyzas, G.Z.; Matis, K.A. Electroflotation process: A review. *J. Mol. Liq.* **2016**, *220*, 657–664. [CrossRef]
4. Madureira, C.M.N. Size, grade and liberation: A stochastic approach to the fundamental problem of mineral processing. In Proceedings of the XVI International Mineral Processing Congress, Stockholm, Sweden, 5–10 June 1988; Elsevier: Stockholm, The Netherlands, 1988; pp. 1823–1834.
5. Sousa, R.; Simons, B.; Bru, K.; de Sousa, A.B.; Rollinson, G.; Andersen, J.; Martin, M.; Leite, M.M. Use of mineral liberation quantitative data to assess separation efficiency in mineral processing—Some case studies. *Miner. Eng.* **2018**, *127*, 134–142. [CrossRef]
6. Liu, L.; Tan, Q.; Liu, L.; Cao, J. Comparison of different comminution flowsheets in terms of minerals liberation and separation properties. *Miner. Eng.* **2018**, *125*, 26–33. [CrossRef]
7. Machado Leite, M.R. Liberation by size reduction. Consequences and improvements on flotation kinetics. In *Innovations in Flotation Technology*; NATO ASI Series E; Springer: Dordrecht, The Netherlands, 1992; pp. 149–170.
8. Gaudin, A.M. *Principles of Mineral Dressing*; McGraw-Hill: New York, NY, USA, 1939.
9. Gay, S. A liberation model for comminution based on probability theory. *Miner. Eng.* **2004**, *17*, 525–534. [CrossRef]
10. Ueda, T.; Oki, T.; Koyanaka, S. Stereological correction method based on sectional texture analysis for the liberation distribution of binary particle systems. *Adv. Powder Technol.* **2017**, *28*, 1391–1398. [CrossRef]
11. Leißner, T.; Mütze, T.; Bachmann, K.; Rode, S.; Gutzmer, J.; Peuker, U. Evaluation of mineral processing by assessment of liberation and upgrading. *Miner. Eng.* **2013**, *53*, 171–173. [CrossRef]
12. Wills, B.A. *Mineral Processing Technology: An Introduction to the Practical Aspects of Ore Treatment and Mineral Recovery*; Butterworth-Heinemann: Amsterdam, The Netherlands, 2011.
13. Zhang, J.; Subasinghe, N. Prediction of mineral liberation characteristics of comminuted particles of high grade ores. *Miner. Eng.* **2013**, *49*, 68–76. [CrossRef]
14. Wills, B.A. Enhancement of minerals liberation. In Proceedings of the 16th International Mineral Processing Congress, Stockholm, Sweden, 5–10 June 1988; pp. 293–297.
15. Lichter, J.; Lim, K.; Potapov, A.; Kaja, D. New developments in cone crusher performance optimization. *Miner. Eng.* **2009**, *22*, 613–617. [CrossRef]
16. Oleg, D.N. *Mechanical Crushing and Grinding*; Elsevier: Amsterdam, The Netherlands, 2019; pp. 65–90.
17. Numbi, B.; Zhang, J.; Xia, X. Optimal energy management for a jaw crushing process in deep mines. *Energy* **2014**, *68*, 337–348. [CrossRef]

18. Parisa, P.; Mehdi, P.; Jan, R. Quantitative analysis of ore texture breakage characteristics affected by loading mechanism: Frag-mentation and mineral liberation. *Miner. Eng.* **2022**, *182*, 107561.
19. Jack, J.; Alex, S. Energy Consumption in Mining Comminution. *Procedia CIRP* **2016**, *48*, 140–145.
20. Farjana, S.H.; Huda, N.; Mahmud, M.P.; Saidur, R. A review on the impact of mining and mineral processing industries through life cycle assessment. *J. Clean. Prod.* **2019**, *231*, 1200–1217. [CrossRef]
21. Kenneth, H.; Päivi, K.-R.; Pirita, H.; Kati, V.; Ali, E. Global energy consumption due to friction and wear in the mining industry. *Tribol. Int.* **2017**, *115*, 116–139.
22. Yongbo, F.; Jiyan, Q.; Shihai, L.; Chun, F. Micron-sized ore powder production by propulsion and rapid unloading of high-pressure gas. *J. Aust. Ceram. Soc.* **2021**, *57*, 1489–1497. [CrossRef]
23. Sajid, M.; Bary, G.; Asim, M.; Ahmad, R.; Ahamad, M.I.; Alotaibi, H.; Rehman, A.; Khan, I.; Yin, G. Synoptic view on P ore bene-ficiation techniques. *Alex. Eng. J.* **2022**, *61*, 3069–3092. [CrossRef]
24. Benredjem, Z.; Delimi, R. Use of extracting agent for decadmiation of phosphate rock. *Phys. Procedia* **2009**, *2*, 1455–1460. [CrossRef]
25. Guo, F.; Li, J. Separation strategies for Jordanian phosphate rock with siliceous and calcareous gangues. *Int. J. Miner. Process.* **2010**, *97*, 74–78. [CrossRef]
26. Houot, R. Beneficiation of iron ore by flotation—Review of industrial and potential applications. *Int. J. Miner. Process.* **1983**, *10*, 183–204. [CrossRef]
27. Dong, X.; Siqing, L.; Yanqing, Y.; Hailin, L.; Yi, P. A review on new technological progress for beneficiation of refractory phosphate ore in China. *IOP Conf. Ser. Earth Environ. Sci.* **2017**, *63*, 012043. [CrossRef]
28. Yang, J.; Qiu, Y. Comparative study on mineral dissemination characteristics of phosphate ores by X-ray micro-computed to-mography and BGRIMM Process Mineralogy Analysis. *Sci. Rep.* **2022**, *12*, 21122. [CrossRef] [PubMed]
29. Zhao, Y.; Long, W.; Huang, S.; Zhong, S.; Shen, Y.; Wang, L. Removal mechanism of oxide film on 304 stainless steel surface by silver brazing flux containing fluoride. *Rare Metal. Mat. Eng.* **2023**, *51*, 4502–4507. [CrossRef]
30. Ji, Q.; Li, G.; Zhu, X.; Gao, T.; Qin, G.; Xu, C.; Cai, M.; Lu, Z.; Chen, Y.; Zhang, J.; et al. Process Mineralogy Automatic Detection System in Research of a Gold Polymetallic Mine. *J. Phys. Conf. Ser.* **2023**, *2428*, 012009. [CrossRef]
31. Ruan, Y.; He, D.; Chi, R. Review on beneficiation techniques and reagents used for phosphate ores. *Minerals* **2019**, *9*, 253. [CrossRef]
32. Ashraf, M.; Zafar, Z.I.; Ansari, T.M. Selective leaching of low grade calcareous phosphate rock in succinic acid. *J. Res. (Sci.)* **2007**, *18*, 145–157.
33. Zhang, G.H.; Fan, Y.B.; Yang, R.S.; Li, S.H. Influence of ore size on the production of micro-sized ore particles by high-pressure gas rapid unloading. *Powder Technol.* **2023**, *427*, 118716. [CrossRef]